10-2009

Volumetric Flank Wear Characterization for Titanium Milling Insert Tools

Uli Burger
Clemson University

Mathew Kuttolamadom
Clemson University

April Bryan
Rose-Hulman Institute of Technology

Laine Mears
Clemson University, mears@clemson.edu

Thomas Kurfess
Clemson University

Proceedings of the 2009 ASME International Manufacturing Science and Engineering Conference
MSEC2009
October 4-7, 2009, West Lafayette, Indiana, USA

MSEC2009-84256

VOLUMETRIC FLANK WEAR CHARACTERIZATION FOR TITANIUM MILLING INSERT TOOLS

Uli Burger
Clemson University – Int'l Center for Automotive Research
Greenville, S.C , USA

Mathew Kuttolamadom
Clemson University – Int'l Center for Automotive Research
Greenville, S.C , USA

April Bryan
Department of Mechanical Engineering
Rose-Hulman Institute of Technology
Terre Haute, IN

Laine Mears
Clemson University – Int'l Center for Automotive Research
Greenville, S.C , USA

Thomas Kurfess
Clemson University – Int'l Center for Automotive Research
Greenville, S.C , USA

KEYWORDS
Machining, Tool Wear, Milling, Titanium, Tool Life

ABSTRACT
Machining wear models are useful for the prediction of tool life and the estimation of machining productivity. Existing wear models relate the cutting parameters of feed, speed, and depth of cut to tool wear. The tool wear is often reported as changes in flank width or crater depth. However, these one-dimensional wear measurements do not fully characterize the tool condition when tools wear by other types of wear such as notching, chipping, and adhesion. This is especially true when machining difficult-to-machine materials such as titanium. This paper proposes another approach for characterizing tool wear. It is based on taking measurements of the retained volume of the cutting tool. The new wear characterization approach is used to demonstrate the progression of volumetric wear in titanium milling.

1.0 INTRODUCTION
Wear models are useful for the estimation of tool life, and the optimization and predictive control of cutting processes. Traditional wear models relate the cutting parameters of speed, feed and depth of cut to the cutting time or cutting length. It is widely accepted that the cutting conditions such as the tool and workpiece geometry, material, and surface finish also significantly affect tool life [1]. One-dimensional measurements of flank wear and crater depth are typically used to quantify the amount of wear at the end of tool life.

In the machining of difficult-to-machine materials such as titanium, other wear mechanisms such as abrasion, chipping, and adhesion may occur. To limit the effects of these types of wear, milling tools have complex geometries that are characterized by a combination of rake and relief angles. The recommended end mills for titanium milling are often much more complex than traditional face and end mills as the low thermal conductivity, low elastic modulus, and high temperature strength of titanium necessitate the use of tools with very high rake and relief angles. Figure 1 shows one such insert.

The complexity of these cutting surfaces and the dominance of wear mechanisms such as abrasion and adhesion make the development of relationships between the geometry of new and worn tools challenging. As a result, the characterization of the geometry and wear of milling tools used for difficult-to-machine materials has lagged behind the characterization of tools used for turning and traditional milling. For these inserts, a volumetric measurement of flank wear has the possibility of offering more insight into the progression of wear than the traditional one-dimensional measurements of crater or flank depth.

FIGURE 1 - TITANIUM MILLING INSERT [2]

In this research, an approach for measuring and characterizing the volumetric wear of milling inserts is proposed. The measurement approach involves capturing a point cloud of data with a white light interferometer and then registering the data to CAD. Volumetric wear is then obtained by comparing the measured volumes of new and worn inserts.

2.0 BACKGROUND

Tool wear, as an input to cost- or time-optimization of process parameters, is an essential factor. Cost and time contribution of wear in titanium machining is especially appreciable due to the adiabatic nature of the shearing process, where the majority of heat generated transfers not to the chip, but instead remains in the tool. This heat buildup causes loss of hardness and accelerated wear of the tool, typically limiting cutting speeds.

2.1 Titanium Machining

Titanium is not as easy to machine as more common materials such as aluminum and steel. Factors contributing to the difficulty in machining titanium are:

- *Low Thermal Conductivity*: The insulation nature of the material restricts more of the heat generated from shearing and friction to the tool's material [3]. Hardness drops with temperature and the tool wears more quickly through plastic deformation and thermal shock cracking mechanisms.

- *Low Elastic Modulus*: The elastic modulus of titanium is half that of steel [4]. This causes excessive workpiece deformation in the cutting zone, as well as detrimental dynamic effects such as chatter, vibration and increased friction during relaxation [4, 5].

- *Chemical Reactivity*: The reactivity of titanium increases at higher temperatures, causing adhesive wear of the tool. As a result, coated tools have much greater rates of adhesive wear once the coating is removed after the initial wear in period [4]. The adhesion effect increases stress during machining and can lead to catastrophic chipping.

- *High Temperature Strength*: The shear strength of titanium is maintained at temperature levels typical of machining, hindering chip formation. The smaller chips formed contact in a smaller area, increasing tool stress at the cutting edge [4,5].

In an effort to reduce cutting forces and lower tool wear, tools with sharp edges, small tool nose radius and high positive rake angles are often recommended for titanium milling [6]. All of these conditions exacerbate tool wear, as these conditions reduce the structural strength for a given tool material. High-speed machining is being investigated as a method of increasing tool life per volume removal [7]. However, temperature does not decrease significantly with HSM, further increasing wear [8].

2.2 Tool Wear Characterization

Wear is traditionally measured as the change in flank depth (VB) or crater depth (KT) as shown in Figure 2. The standard measure for the end of life for milling tools is a uniform average flank depth over all the teeth of 0.3mm and a localized wear depth of 0.5mm [10].

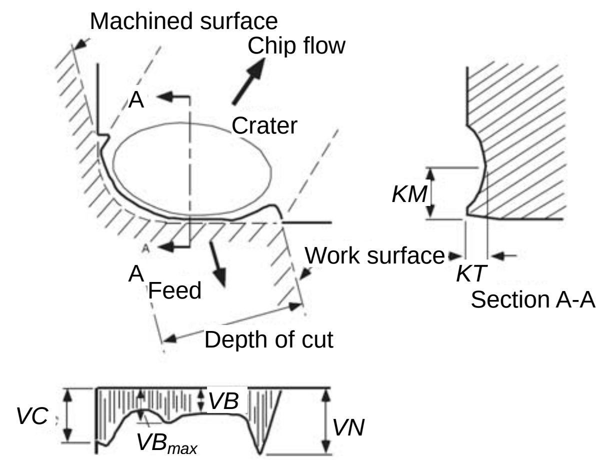

FIGURE 2 – TRADITIONAL WEAR MEASUREMENTS [11]

Cutting tool wear models, such as the fundamental Taylor tool life equation Eq. (1), predict this end of tool life by relating the cutting parameters to the cutting time. In the Taylor's equation, *V* represents cutting speed in m/min, *T* represents usable life in min, and *n* and *C* are process-specific constants, derived from empirical data. However, due to the difference in wear mechanisms, the wear curves for titanium milling do not always agree with Taylor's tool life equation.

$$VT^n = C \quad (1)$$

Other models that consider cutting materials, such as material flow stress models accurately represent tool strength [12,13]. However, these models are not typically used to predict tool wear.

2.3 Volumetric Tool Wear

Flank width (VB) and crater depth (KT) shown in Figure 2 are one-dimensional measurements of tool wear. Stereomicroscopes, which were readily available at the time these measurement techniques were introduced, are often used to measure VB and KT. Measurements of VB and KT are representative of the worst wear conditions experienced when a carbide tool is used to machine steel [11].

However, flank or crater wear are not the primary wear mechanisms for some combinations of workpiece and tool. materials For example, notch wear dominates when ceramic tools are used to machine nickel [11], and micro-chipping and adhesive wear dominate when carbide tools are used to machine titanium [1, 11]. For these latter cases, flank wear and crater depth may be relatively low even when the tool is near failure. Therefore, these wear measurements do not sufficiently capture the wear observed in these latter situations.

In addition, VB was initially assumed to change linearly over time. However, more recent researchers have proposed non-linear models for flank wear. Dawson and Kurfess [14] used a model based on volumetric wear measurements of a prismatic turning tool to show the relationship between these linear and non-linear wear models.

The premise of this work is that wear can be more accurately characterized by a volumetric quantification. As opposed to the linear measures of VB and KT, volumetric wear measurements indicate the quantity of material lost from the cutting region. The measurement of volumetric wear is independent from the dominant wear mechanism. Therefore, volumetric wear values can provide a better understanding of imminent tool failure. Our objective in this research is to volumetrically characterize complex milling tool geometries, and use the data obtained via titanium cutting experiments across a range of feed and speed to ascertain the progression of wear using this new volumetric measurement approach.

3.0 CHARACTERIZATION OF VOLUMETRIC WEAR

The approach undertaken for characterizing tool wear is one in which a volumetric quantification of the cutting contact area of the worn inserts is obtained and compared to that of an unworn insert.

As a starting point, profile measurements of the area of interest for each of the cutting inserts are performed using a displacement measuring interferometer. The Zygo NewView 7200 3D Surface Profiler capable of mapping surface variations as small as 10^{-10} m was employed for this purpose to accurately record the flank region geometry of the worn and unworn tool inserts. From these investigations, accurate point cloud data of insert geometries were derived in the form of '.xyz' data files. Following this, these data files were imported into a 3D scanning/processing software for further analyses. RapidForm XORedesign, capable of generating parametric CAD models from 3D scan data was the software used to convert and enhance these point cloud data files obtained from the 3D surface profiler. Figure 3 shows an example of the initial point cloud map of an insert after initial cleaning.

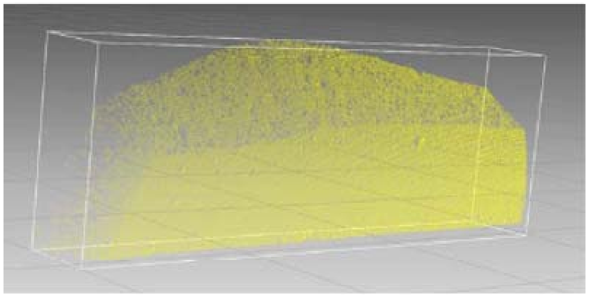

FIGURE 3 - INITIAL POINT CLOUD OF DATA AFTER CLEANING PROCESSES

As stated, using the 3D scanning/processing software, the point cloud data set is cleaned of most of the noise so as to prepare it for further processing. Following this, a preliminary surface is fitted over the data points as shown in Figure 4.

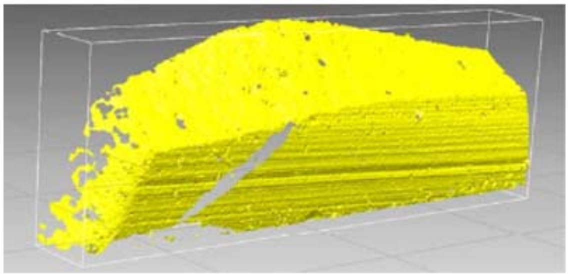

FIGURE 4 - PRELIMINARY SURFACE FITTED OVER DATA POINTS

The fitted surface is further processed using the RapidForm software in order to obtain a closed geometry that is free from holes, with fairly well defined boundaries. Following this, the powerful 3D processing software capabilities enable the triangulation/merging, healing, enhancing and smoothing of the surface data. A mesh buildup is performed on this surface data and this mesh is optimized to obtain a model that accurately represents the surface characteristics of the worn/unworn flank region geometry. The result of the above processes for the unworn flank geometry is shown in Figure 5. The elements generated are closely comparable to the models used for finite element analysis. The high quality of the surface models thus obtained enables them to be exported as standard CAD file formats.

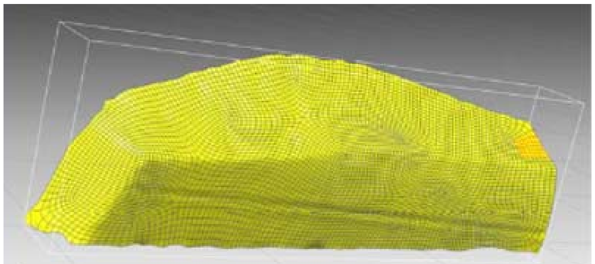

FIGURE 5 - MESHED SURFACE, EXPORTABLE TO COMMON CAD-FILE-FORMATS

The so derived surface model is further processed using common CAD software. The generative shape design workbench of CATIA V5 was utilized to further process the imported surface models as this software has the capability to manage models with multiple surfaces. Any defects that could not be fixed using RapidForm are repaired after importing the model into CATIA. The surface model after importing and repairing it is shown in Figure 6.

FIGURE 6 - SOLID MODEL OF INSERT FOR VOLUME MEASUREMENT

Using the CAD software, a representative volume of the cutting edge geometry of each insert is derived via several steps. This predominantly involves matching certain geometric elements identified initially, such as the marked corners of the worn and unworn inserts, so that a consistent reference basis for volume measurements is maintained. Based on surface models obtained from initial point cloud data and the insert geometry information provided by the insert manufacturer (Iscar [2]), the solid models of the unworn and worn inserts are designed and matched with the aid of drafting some well defined construction elements such as a cutting edge line, certain planes at specific angles, etc. The relative volumes of these models were thus measured satisfactorily and compared for each case while maintaining a consistent basis for all machining experiments.

4.0 EXPERIMENTAL APPROACH

Experiments are used to determine the progression of volumetric wear for titanium milling. The geometries of new and worn inserts are measured by the new volumetric approach presented in Section 3. The experimental design is shown in Table 1. From the table, it can be seen that wear is recorded at two levels of feeds and speeds. The depth-of-cut was held constant at 2.0mm. No coolant was used for these experiments.

TABLE 1 - EXPERIMENTAL DESIGN

Experiment	Design		Parameters	
			Speed (m/min)	Feed (mm/rev)
1	+	+	200	0.5
2	+	-	200	0.2
3	-	+	70	0.5
4	-	-	70	0.2

The experiments were performed on an Okuma MB-46 3-axis vertical mill. The workpiece material was Ti-6Al-4V. Helmill HM90 APCR 100304PDFR-P/DP carbide inserts with a TiAlN coating were used. The tool holder was one inch in diameter and could hold up to four indexable inserts [2]. All four inserts were used in the tool holder for each experiment in Table 1. The inserts had a 28^o positive rake angle. Figure 1 is a picture of one of the inserts used

Three milling passes were used for each experiment shown in Table 1. Each milling pass was a shoulder cut 12.7mm wide and 154.8mm long. Therefore, each insert was used for a total cut length of 464.4mm. The volume in the cutting region of each insert was recorded four times for each experiment, once before machining and after each of the three milling passes.

As stated in Section 3, the measurements were recorded with the Zygo NewView 7200 white light interferometer. A fixture was used to hold the insert in place on the interferometer's stage. Chips or loose material that could be removed with the thumb were brushed away before measurement as described in the ISO milling standard [10]. However, no other formal cleaning process was used. In addition, a stereomicroscope was used to capture actual images of the insert for wear mechanism analysis.

5.0 RESULTS

5.1 Wear Characterization Results

This section describes the implementation of the volumetric wear characterization process outlined in the previous section. Sample inserts tested under the conditions specified in Experiment 1, i.e. speed=200m/min and feed= 0.5mm/rev, are used as an example. Unlike the inserts in Experiment 1 that were used to a maximum length of 464.4mm, these inserts were used until failure.

Figure 7a shows a microscope image of the flank face of an unworn insert at 40X magnification. Figure 7b shows the corresponding solid model (in purple) of the flank region of the same insert with the reference surface model (as the yellowish surface) superimposed on top of it. As could be observed from Figure 7 and the following figures in this sub-section, only the top part of the flank region (region between the cutting edge line and the line separating the surface containing the flank face with the remaining body of the insert, that are almost parallel to each other) was investigated for the volumetric measurement as this is the only portion in contact with the work piece within normal wear limits. Hence, the solid model has been trimmed accordingly to only constitute the portion of interest.

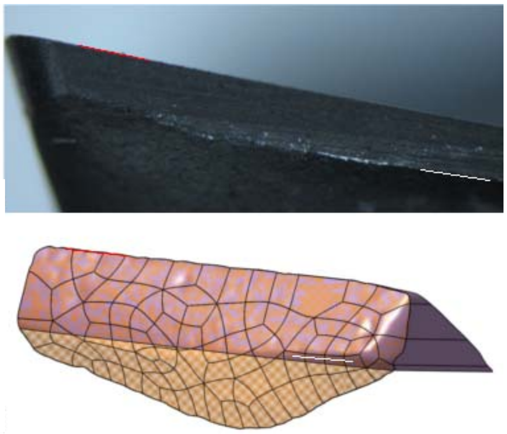

(A)

(B)

FIGURE 7 - UNWORN INSERTS, A) MICROSCOPE IMAGE AND B) SOLID MODEL FOR MEASUREMENTS ALONG WITH REFERENCE SURFACE

Figure 8 further illustrates some relevant steps during the matching process between the unworn and worn inserts. As can be seen in Figure 8, the unworn reference surface was retained during the comparisons with worn surface models for the correct determination of the worn flank region volume during the machining experiments. Figure 8a depicts the matching procedure between a worn and unworn surface after a cutting length of 154.8 mm (Experiment 1, Step 1) for one of the four inserts (green surface model is the worn insert surface and orange surface model is the unworn reference insert surface) and Figure 8b shows the solid model created after attaining correct matching.

Note how the worn and unworn surfaces have been matched closely (to be as coincident as possible) in Figure 8a by aligning the left edges in the figure as well as the (almost horizontal in the figure) line separating the surface containing the flank face with the remaining body of the insert. Some portions of the worn surface extend beyond the reference surface in Figure 8a – this is attributed to the thermal distortion of the insert.

In Figure 9, the microscopic image of one of the used inserts and the corresponding solid model for one of the inserts are shown after a cutting length of 154.8 mm (Experiment 1, step 1). The reference surface of the unused insert shown above in Figure 7b was used as a reference to ensure that the right region was selected for modeling. It is not shown in the following figures.

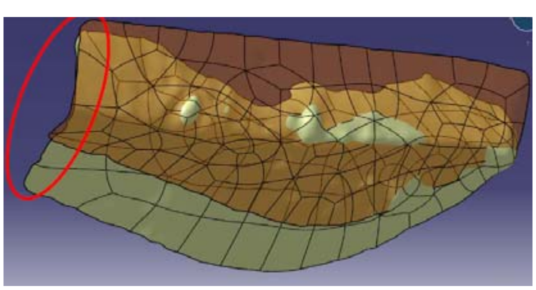

(A)

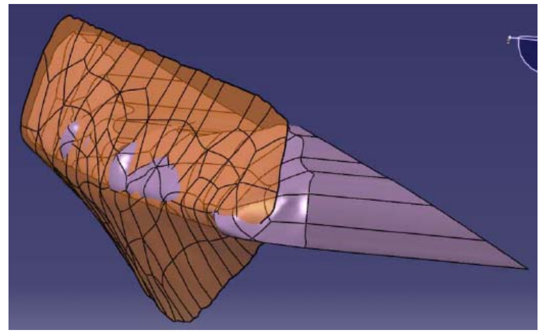

(B)

FIGURE 8 - MATCHING PROCESS, A) SURFACE MATCHING BETWEEN WORN AND UNWORN SURFACES AND B) SOLID MODEL OF WORN INSERT WITH UNWORN REFERENCE SURFACE

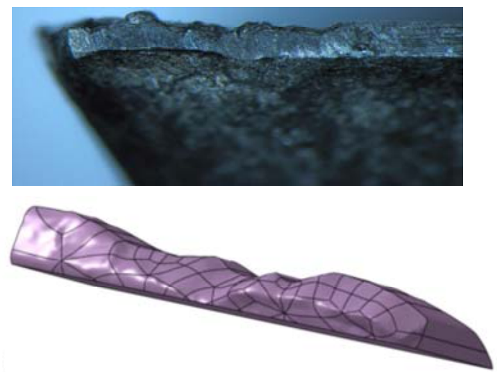

(A)

(B)

FIGURE 9 - INSERT AFTER A CUTTING LENGTH OF 154.8 MM, A) MICROSCOPE IMAGE AND B) SOLID MODEL FOR VOLUMETRIC COMPARISON

Following through in this manner, a microscopic picture and the related solid model are shown in Figure 10 after a cutting length of 309.6 mm (end of step 2). As could be clearly observed in both sub-images, the wear stage has further progressed. The solid model for volumetric quantification was derived in the same way as before.

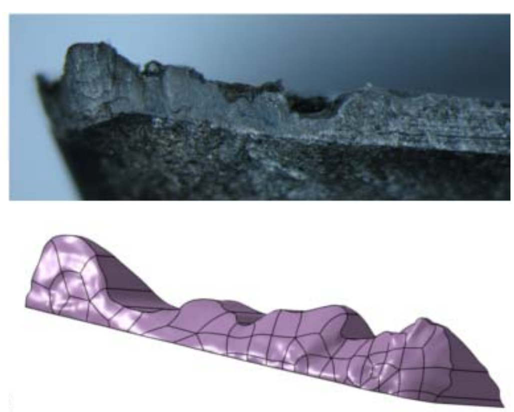

(A)

(B)

FIGURE 10 - INSERT AFTER A CUTTING LENGTH OF 309.6 MM, A) MICROSCOPE IMAGE AND B) SOLID MODEL USED FOR VOLUMETRIC COMPARISON

Figure 11 shows again a microscopic picture of the same insert together with the solid model recorded after a cutting length of 464.4 mm (end of step 3). Besides even further progression of wear, note how the wear stage has progressed beyond the line separating the surface containing the flank face with the remaining body of the insert that was intact until now.

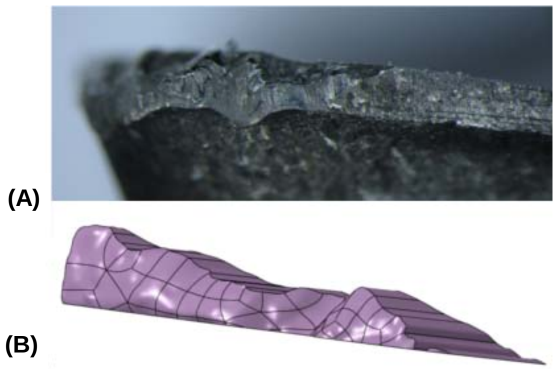

FIGURE 11 - INSERT AFTER A CUTTING LENGTH OF 464.4 MM, A) MICROSCOPE IMAGE AND B) SOLID MODEL USED FOR VOLUMETRIC COMPARISON

Thus, following the quantification process outlined above, the results of the relative volume measurements of the solid models could be used to compare the tool wear at different steps and experiments to the unworn insert at any stage of wear.

5.2 Machining Effect on Tool Wear

5.2.1 Wear Data

The volumetric wear characterization procedure outlined in Section 3 was used to determine the wear volumes of each of the inserts used in each of the four machining experiments described in Section 4. At each cutting interval, the point cloud of data obtained from the white light interferometer was used to determine the retained volume of the insert. The volumetric wear of the insert was then computed by subtracting the retained volume of the insert from the average volume of four unworn reference inserts as shown in Eq. (2).

$$VW = \frac{\sum_{i=1}^{4} Volref_i}{4} - Vol \qquad (2)$$

VW is the worn volume of the insert of interest, Vol is the retained volume of the insert of interest after machining, and $Volref_i$ is the volume of the unworn reference insert i. The average volume in the flank region of the four unworn inserts was found to be 6.147mm^3.

The average volumetric wear of the four inserts on the tool was calculated at the end of each cutting length for each experiment. Table 2 gives a summary of the average volumetric wear measurements for each of the cutting intervals for all four experiments. As the inserts used in Experiment 4 experienced catastrophic failures before the end of the first cutting interval, no volumetric wear results are reported for this experiment.

TABLE 2 - VOLUMETRIC WEAR RESULTS

Cutting Length (mm)	Average Volumetric Wear Across 4 Inserts (mm^3)			
	Experiment 1	**Experiment 2**	**Experiment 3**	**Experiment 4**
	V=200m/min	V=70m/min	V=200m/min	V=70m/min
	f=0.5mm/rev	f=0.2mm/rev	f=0.2mm/rev	f=0.5mm/rev
154.8	1.285	0.046	0.057	No Data / Tool Failure
309.6	1.955	0.118	0.305	
464.4	3.472	0.274	0.807	

Figures 12a-b are plots of the volumetric wear data given in Table 2. The plot in Figure 12a shows the average volumetric wear in mm^3 versus feed at the end of each cutting interval for a fixed speed of 200m/min. While the plot in Figure 12b shows the average volumetric wear in mm^3 versus speed at the end of each cutting interval for a fixed feed of 0.2mm/rev.

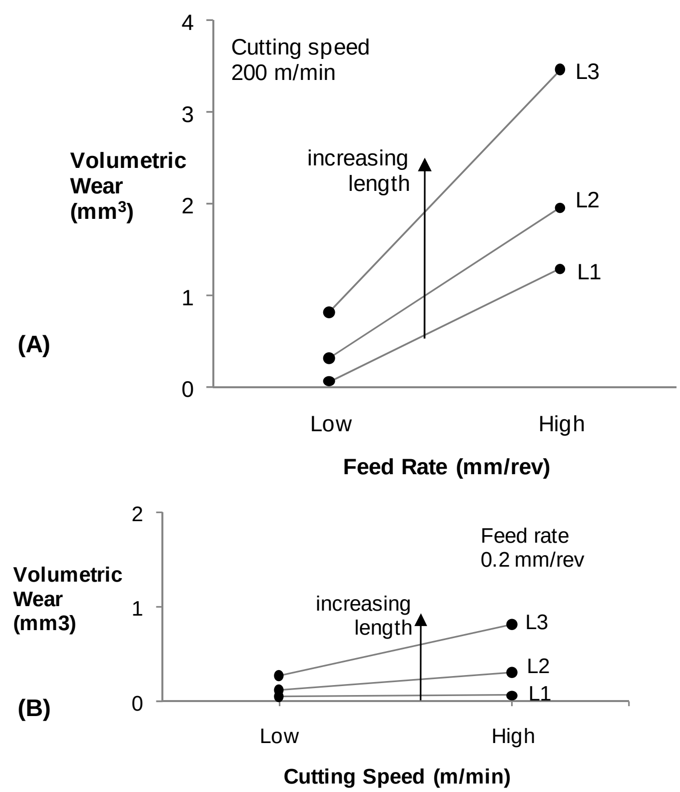

FIGURE 12 – A) AVERAGE VOLUMETRIC WEAR VS FEED FOR EXPERIMENTS 1-3 B) AVERAGE VOLUMETRIC WEAR VS SPEED FOR EXPERIMENTS 1-3

As expected, the average volumetric wear of the inserts increase monotonically with cutting length as shown in Table 2 and Figures 12a-b. The results in Table 2 and Figure 12b also confirm that the cutting speed and feed have a significant influence on wear, i.e. the volumetric wear increased as speed and feed increased. It is also noted that the feed had a greater influence on volumetric wear than the cutting speed. Additional experiments are required to determine the mathematical relationship between the cutting time and volumetric wear measurements.

The lowest wear was obtained with the cutting conditions of low speed and feed used for Experiment 2. The least favorable wear results were obtained with the combination of high feed and low speed used in Experiment 4. This was the experiment that resulted in catastrophic tool failure. These results are consistent with wear results previously obtained in the literature [1,4].

In general, the volumetric wear curves of individual inserts were consistent with Figure 12 showing monotonically increasing wear. However, there were occasions when the volumetric wear of an individual insert was lower after one cutting interval than the previous interval. This wear phenomenon was especially pronounced in Experiment 2, the experiment with the lowest volumetric wear. Figure 13 shows the volumetric wear for individual inserts from Experiment 2. From Figure 13, it can be seen that the volumetric wear of insert 1 is larger at the end of the first cutting length than at the end of the second and the volumetric wear of insert 3 is larger after the end of the second cutting length than at the end of the third. Due to space limitations, the CAD models representing these volumetric wear trends have not been included. They can be obtained from the authors upon request.

One possible cause of this unusual volumetric wear could be abrasion and adhesion of chips during machining. Images of the flank region of the inserts at the end of test show the presence of these wear mechanisms, Figure 14. Traditional one-dimensional measures of flank wear and crater depth would not be able to characterize this phenomenon.

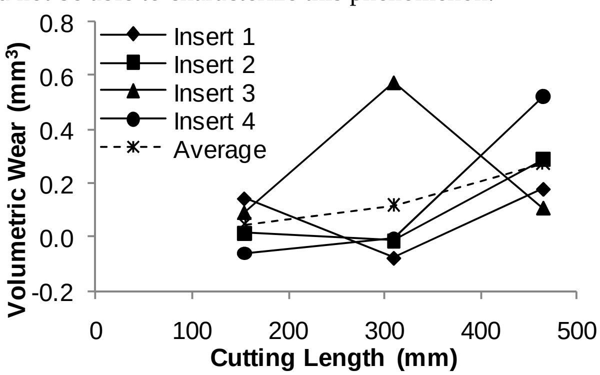

FIGURE 13 - VOLUMETRIC WEAR PLOTS FOR INDIVIDUAL INSERTS IN EXPERIMENT 2

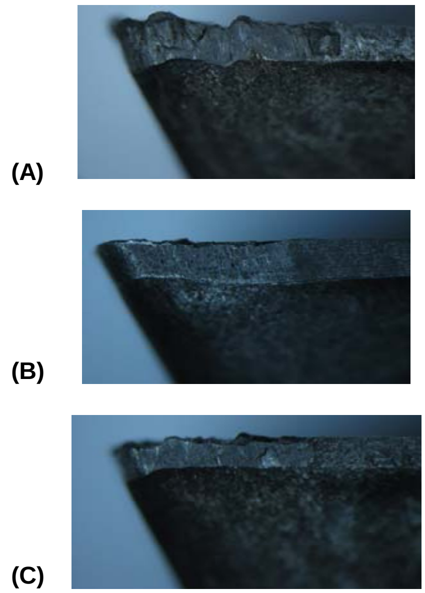

FIGURE 14 – INSERT CONDITION AT THE END OF TEST FOR: A) EXPERIMENT 1, B) EXPERIMENT 2 AND C) EXPERIMENT 3

5.2.2 Wear Mechanism

Images showing the conditions of the inserts at the end of Experiments 1-3 are shown in Figures 14a-c. Figure 9a, Figure 10a and Figure 11a show the conditions of the inserts from the trial run at three cutting intervals. It is noted that the inserts in these latter figures were used until failure and the cutting intervals are not the same as the one in the experimental design. These images were recorded with a stereomicroscope at 40x magnification.

The insert images show that the dominant wear mechanisms were abrasion, micro-chipping and adhesion. They also indicate the lack of significant flank wear and notching. The highest flank wear was observed with Experiments 1 and 4, the experiments with high speed. The inserts from the trial experiment, which had the same machining conditions as Experiment 1, also showed signs of flank wear as shown in Figures 11a and 12a. There are almost no signs of flank wear on the inserts used for Experiments 2 and 3. As the images were taken without a scale, the exact values for flank wear are not reported.

6.0 CONCLUSIONS

A volumetric measurement approach was introduced as a new procedure for characterizing the wear geometry of milling inserts. The approach was used successfully to determine the progression of wear when milling titanium. The wear volumes of inserts were obtained by comparing the solid models of worn inserts with that of an unused insert. The solid models, which were obtained from point clouds of data acquired with a white light interferometer, showed good comparative geometry with the actual tool inserts.

The results for the volumetric wear indicated that among the conditions tested, the best cutting conditions for dry milling titanium with carbide inserts are a combination of low speed and low feed (70m/min., 0.2mm/rev). These results are consistent with other machining models. The volumetric wear curves are not consistent with the wear curves obtained by measuring a single dimension of wear such as flank depth. Further analysis is required to determine the relationship between the flank depth and volumetric wear.

7.0 FUTURE WORK

The experiments performed in this study were used to obtain an understanding of the progression of volumetric wear in titanium milling. They were sufficient to obtain a qualitative understanding of the progression of volumetric wear but not to establish mathematical relationships.

In the future, more detailed experiments for the purpose of building mathematical relationships of the progression of volumetric wear over time will be performed. The mathematical models obtained from these experiments will be used for the prediction of wear and optimization of the cutting process for new combinations of tool and workpiece material, tool geometries and cutting conditions.

ACKNOWLEDGEMENTS

The authors would like to thank Richard Layton, who is an Associate Professor of Mechanical Engineering at Rose-Hulman Institute of Technology, for his assistance with data representation.

8.0 REFERENCES

[1] Wang, Z. G., Rahman, M., and Wong, Y. S. (2005). "Tool wear characteristics of binderless CBN tools used in high-speed milling of titanium alloys." *Wear*, 258(5-6), pp. 752-758.

[2] Iscar Corp. (2009). "Milling Tools Catalog." <www.icar.com>.

[3] Konig, W., Tondorf, J., and Bouzakis, K. (1979). "Possibilities to avoid built-up edges in gear hobbing." *Annals of the CIRP*, 28(1), pp. 77-81.

[4] Ezugwu, E. O., and Wang, Z. M. (1997). "Titanium alloys and their machinability - a review." *Journal of Materials Processing Technology*, 68(3), pp. 262-274.

[5] Yang, X., and Liu, C. R. (1999). "Machining titanium and its alloys." *Machining Science and Technology*, 3(1), pp. 107-139.

[6] Sandvik Coromant (2008). "Application guide: titanium machining." pp. 185.

[7] Rahman, M., Wang, Z. G., and Wong, Y. S. (2006). "A review on high-speed machining of titanium alloys." *JSME International Journal, Series C (Mechanical Systems, Machine Elements and Manufacturing)*, 49(1), pp. 11-20.

[8] Muller-Hummel, P., and Lahres, M. (1994). "Infrared temperature measurement on diamond-coated tools during machining." *Diamond and Related Materials*, 3(44), pp. 765-9.

[9] Gu, J., Barber, G., Tung, S., and Gu, R.-J. (1999). "Tool life and wear mechanism of uncoated and coated milling inserts." 1999 12th *International Conference on Wear of Materials*, 225-229, pp. 273-284.

[10] International Standards Organization, (1989). "Tool life testing in milling – Part 2 End Milling." *ISO 8688-2*, Geneve Switzerland.

[11] Childs, T., Maekawa, K., Obikawa, T., and Yamane, Y. (2000). Metal Machining: theory and applications. xc*Arnold*, London, Great Britain.

[12] Nouari, M., and Ginting, A. (2007). "Optimal cutting conditions when dry end milling the aeroengine material Ti-6242S." *Journal of Materials Processing Technology*, 184(1-3), pp. 319-24.

[13] Calamaz, M., Coupard, D., and Girot, F. (2008). "A new material model for 2D numerical simulation of serrated chip formation when machining titanium alloy Ti-6Al-4V." *International Journal of Machine Tools and Manufacture*, 48(3-4), pp. 275-88.

[14] Dawson, T. G., and Kurfess, T. R. (2006). "Modeling the progression of flank wear on uncoated and ceramic-coated polycrystalline cubic boron nitride tools in hard turning." *Transactions of the ASME. Journal of Manufacturing Science and Engineering*, 128(1), pp. 104-109.

